IEEE Photonics Journal
An IEEE Photonics Society Publication

Open Access

Simultaneous Measurement of Curvature and Temperature Based on Mach–Zehnder Interferometer Comprising Core-Offset and Spherical-Shape Structures

Volume 8, Number 1, February 2016

Huaping Gong
Mengling Xiong
Ziheng Qian
Chun-Liu Zhao
Xinyong Dong

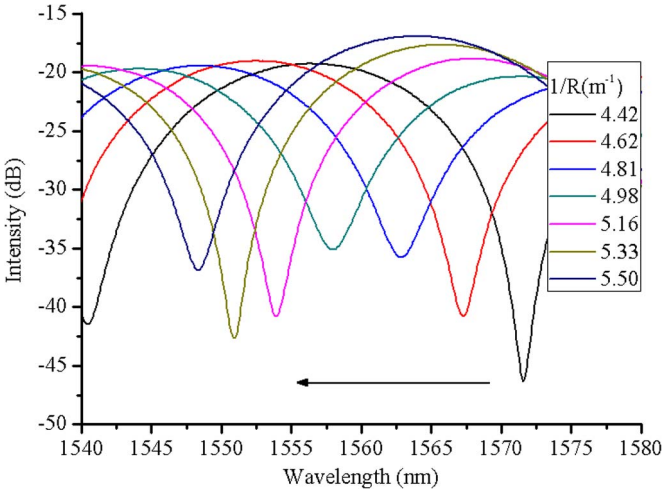

DOI: 10.1109/JPHOT.2015.2500888
1943-0655 © 2015 IEEE

IEEE photonics SOCIETY

IEEE

Simultaneous Measurement of Curvature and Temperature Based on Mach–Zehnder Interferometer Comprising Core-Offset and Spherical-Shape Structures

Huaping Gong, Mengling Xiong, Ziheng Qian, Chun-Liu Zhao, and Xinyong Dong

College of Optical and Electronic Technology, China Jiliang University, Hangzhou 310018, China

DOI: 10.1109/JPHOT.2015.2500888

Manuscript received September 24, 2015; revised November 9, 2015; accepted November 11, 2015. Date of publication December 4, 2015; date of current version December 22, 2015. Corresponding author: H. Gong (e-mail: gonghp77@hotmail.com).

Abstract: A novel sensor for simultaneous measurement of curvature and temperature based on the Mach–Zehnder interferometer (MZI) is presented. The sensor consists of slight core-offset and spherical-shape structures. The core offset excites cladding modes, and the spherical shape couples the cladding modes back into the core and interferes with the core mode. Two dips of the interference fringe shift with the variation of curvature or temperature, and simultaneous measurement of curvature and temperature can be realized by means of a sensitivity coefficient matrix. Two MZIs with different lengths are fabricated. For sensor 1 with the length of 20 mm, the curvature sensitivity is as high as –22.227 nm/m^{-1} in the range of 4.66–5.50 m^{-1}, and the temperature sensitivity is 0.0847 nm/°C in the range of 60 °C–100 °C. For sensor 2 with the length of 16 mm, the curvature sensitivity is –20.128 nm/m^{-1} in the range from 5.66 to 6.53 m^{-1}, and the temperature sensitivity is 0.0737 nm/°C in the range from 40 °C to 100 °C.

Index Terms: Mach–Zehnder interferometer (MZI), spherical-shape structure, core-offset, coefficient matrix, simultaneous measurement.

1. Introduction

The optical fiber sensor has been widely studied because it has the advantages of small size, flexibility, resistance to electromagnetism, and the possibility of distributed measurement. Optical fiber interferometer sensors, especially the Mach–Zehnder interferometer (MZI), have attracted great attention for their application prospects in various areas such as physical measurements, environmental industry monitoring, and chemical measurements, for example, sensors for displacement and force measurements constructed by two S-bend fibers [1], sensors for temperature measurement which applies offset splicing configuration and Germania-doped few-mode fiber [2], and refractive index (RI) measurement based on single-mode-multi-mode-single-mode (SMS) configuration which uses etched multimode fiber (MMF) [3]. Optical fiber curvature sensors have drawn special attentions due to their applications in bending measurement areas [4]. So far, there are various configurations of MZI to realize curvature measurement. We once demonstrated a MZI based on two peanut-shape structures, and the curvature sensitivity is –21.87 nm/m^{-1} [5]. Zhang presented a bending sensor based on lateral-offset

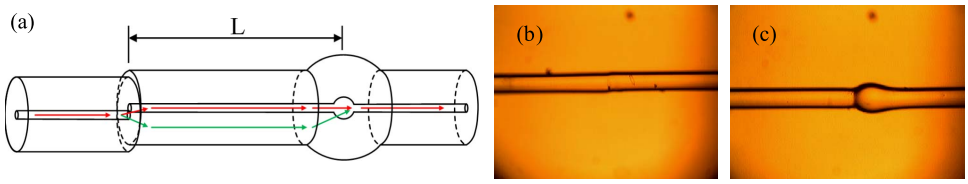

Fig. 1. (a) Schematic diagram of the MZI. (b) Core-offset. (c) Spherical-shape structure.

and up-taper, where the bending sensitivity is 11.987 nm/m^{-1} [6]. L. Niu proposed a curvature sensor based on two cascading abrupt-tapers configuration and the curvature sensitivity of –25.946 nm/m^{-1} is obtained [7]. However, the interference from the other parameters to the bending measurement is a crucial issue, for instance, temperature. Therefore, there are several works about simultaneous measurement of curvature and temperature. Mao presented a MZI for simultaneous measurement of curvature and temperature based on lateral-offset splicing and ultra-abrupt taper [8]. Zhou proposed a sensing structure constructed by combining a PCF-based MZI with a FBG [9], but their curvature sensitivities need to be improved.

In this work, we propose a MZI comprising slight core-offset splicing and spherical-shape structures for simultaneous curvature and temperature measurement. The mode fields of the core-offset junction with different offset values and spherical-shape structure with different diameters are simulated. Two MZIs with different lengths are fabricated, and the responses of curvature and temperature are presented. The best curvature sensitivity of –22.227 nm/m^{-1} is acquired in the range of 4.66–5.50 m^{-1} for the sensor with length of 20 mm. Simultaneous measurement of curvature and temperature can be realized by substituting the sensitivities to coefficient matrix. The slight core-offset splicing can maintain the robustness of the MZI, and the proposed MZI is characterized by high curvature sensitivity, easy fabrication, and good robustness.

2. Sensor Design and Fabrication

The schematic diagram of the proposed MZI for curvature and temperature measurement is depicted in Fig. 1(a). It cascades a lateral core-offset with a spherical-shape structure. The core-offset and the spherical-shape structures are fabricated by commercial fusion splicer (FSM 60S). The spherical-shape structure is fabricated by manual splicing. First, apply arc discharge twice at one end of a single mode fiber (SMF), the end of SMF will be soften and become spherical-shape, the parameters of the arc discharging are as follows: the discharge duration is 1200 ms; the discharge intensity is 135 bit. Second, a section of SMF is spliced to the spherical-shape by normal splicing after manual alignment. The core-offset structure is also fabricated by manual splicing. Two ends of SMF were misaligned with a lateral 8 μm core-offset manually, and then the two ends are spliced together by arc discharge with discharge time of 1700 ms, and discharge intensity of 150 bit. When manufacturing the core-offset structure, radial displacement of 8 μm is measured by proportion method before splicing, and then, it is measured accurately by a microscope after the structure is fabricated.

The simulation of the propagation of the fiber core mode by Rsoft software is depicted in Fig. 2. The operation wavelength is 1550 nm. Fig. 2(a) shows the simulation of light passing through the core-offset structure, and the offset value is set as 8 μm. As the light propagates, it can be observed that about 70% of the light in the fiber core leaks to the cladding. The relationship between the sphere diameter and the output power is plotted in Fig. 2(b), it can be seen that the intensity of the output power will decrease as the offset value increase. Fig. 2(c) shows the propagation of the light at the spherical-shape structure, and the diameter of the sphere is set as 186 μm. It can be seen that about 10% the light in the fiber core leaks to the cladding at the spherical-shape structure. The relationship between the sphere diameter and the output power is shown in

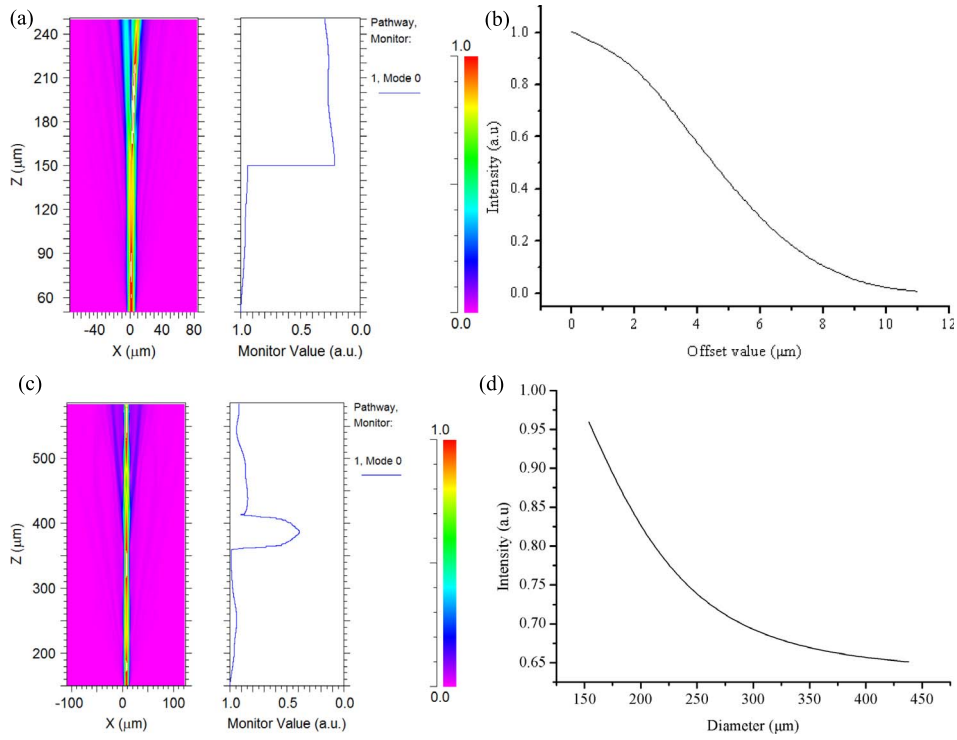

Fig. 2. (a) Simulation of the light propagation of the core-offset structure. (b) Relationship of the offset value and output power intensity. (c) Simulation of the light propagation of the spherical-shape structure. (d) Relationship between the diameter of the spherical-shape structure and the output power.

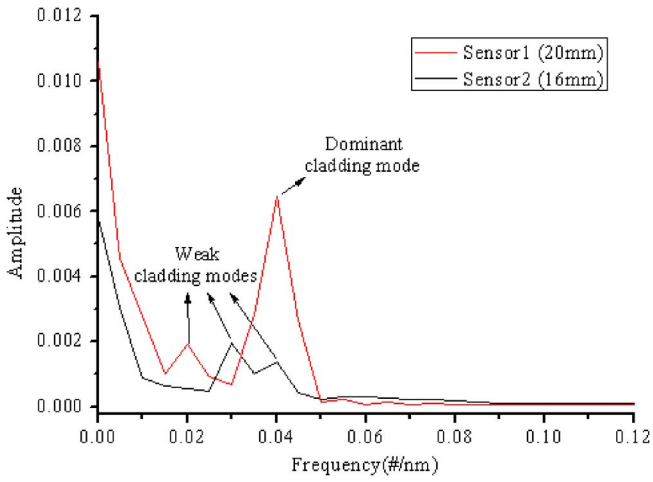

Fig. 3. Spatial frequency spectra of sensor 1 (20 mm) and sensor 2 (16 mm).

Fig. 2(d), as the diameter of the sphere increase, the intensity of the output power will decrease. The simulation results provide a reference for fabricating the sensors.

We fabricated two MZIs with different lengths of 20 mm and 16 mm and named them sensor 1 and sensor 2, respectively. The photo of the core-offset we fabricated is shown in Fig. 1(b), and the offset is 8 μm. The photo of the spherical-shape structure is shown in Fig. 1(c), and the diameter of the sphere is 186 μm. The extinction ratio of the MZI's interference fringes is very high, which can satisfy the demand of measurement. The transmission spectra of sensor 1 (20 mm) and

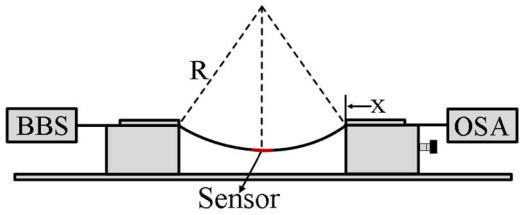

Fig. 4. Experimental setup for curvature measurement.

sensor 2 (16 mm) are measured. The spectra are analyzed by fast Fourier transform (FFT), and the corresponding spatial frequency spectra are shown in Fig. 3. It can be observed that there is one dominant cladding mode and one weak cladding mode for sensor 1, while there are two weak cladding modes for sensor 2, which means sensor 1 excites dominant cladding mode more efficiently.

3. Working Principle and Experiment

As depicted in Fig. 1(a), the input light propagates in the lead-in SMF as core mode. The lateral core-offset junction works as a coupler and the spherical-shaped structure works as a recoupler. The cladding mode will be stimulated at the core-offset junction because of the mismatch of the mode field, and the spherical-shaped structure recombine the core-mode and the cladding mode together, thus an in-line MZI is formed. There is refractive index (RI) difference between the core mode and cladding mode, so it induces the phase difference between the two modes, which can be expressed as

$$\Phi^m = \frac{(2\pi \Delta n_{\text{eff}} L)}{\lambda} \tag{1}$$

where Δn_{eff} is the effective RI difference between the core mode and the cladding mode, L is the length between the core-offset and the spherical-shape structures, and λ is the input wavelength. When the phase difference satisfies the equation $\Phi^m = (2m+1)\pi$, where m is an integer, the interference fringe will show resonance.

When the MZI is bent, the wavelengths of the dips can be given by [5]

$$\lambda_m \cong \frac{\Delta n_{\text{eff}}^0 \cdot L}{2m+1} + \frac{kLd}{2m+1} \cdot \frac{1}{R} \tag{2}$$

where Δn_{eff}^0 is the effective RI difference between the core mode and the cladding mode without bending; $k = -0.1649 \times 10^{-9} \mu\varepsilon^{-1}$ is the strain-RI index coefficient; d is the distance between the fiber core and cladding; R is the bending radius.

According to (2), the dip wavelength is linear to the curvature of the fiber. The wavelength shift of the interference dip can be expected to observe in curvature sensing.

The experimental setup for curvature measurement is shown in Fig. 4. Light from a broadband source (BBS) with the wavelength range from 1500 nm to 1600 nm is put into the MZI. An optical spectrum analyzer (OSA) with a resolution of 0.02 nm is used to monitor and record the transmission spectra of the MZI. The two ends of the MZI are clamped on two translation stages, and the distance between the two translation stages is 150 mm. One of the translation stages is fixed and the other translation stage is moved inward 0.25 mm each time. Therefore, the fiber will be bent and the curvature can be approximately expressed by [10]

$$C = \frac{1}{R} \cong \sqrt{24x/L_0^3} \tag{3}$$

where x is the moving distance of the movable stage, and $L_0 = 150$ mm is the initial separation of the translation stages.

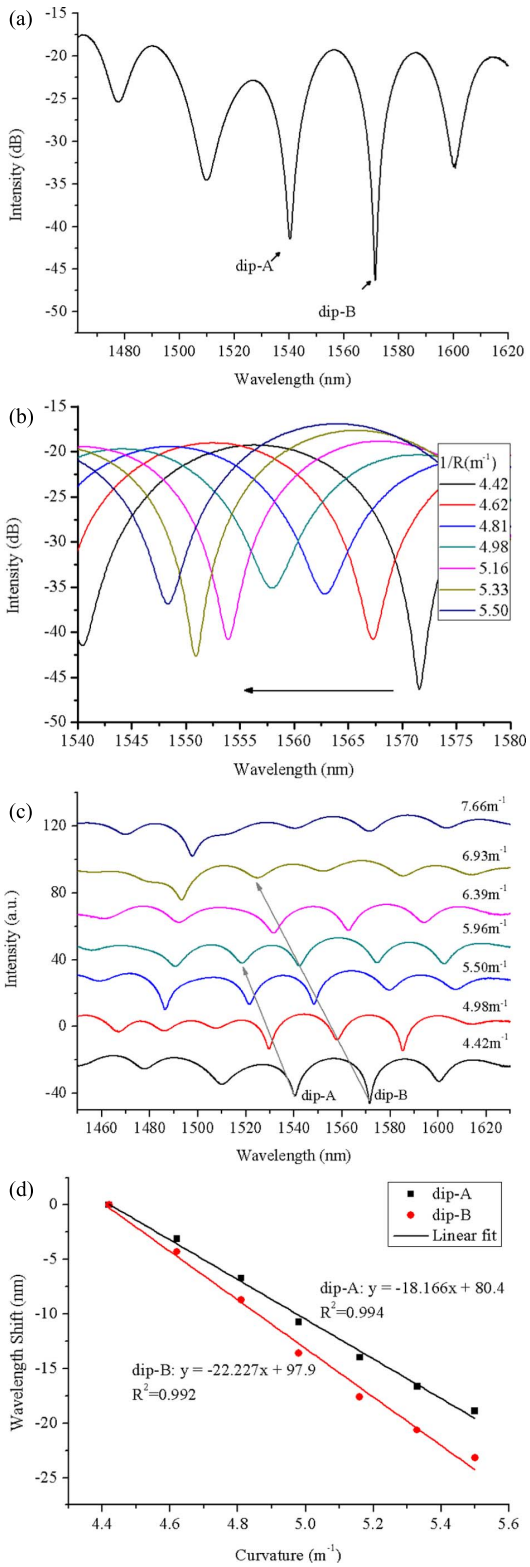

Fig. 5. (a) Transmission spectra of the sensor 1 at the curvature of 4.42 m^{-1}. (b) Wavelength shift of dip-B at different curvatures. (c) Variations of dip-A and dip-B with different curvatures. (d) Wavelength shift of dip-A and dip-B versus the curvature change.

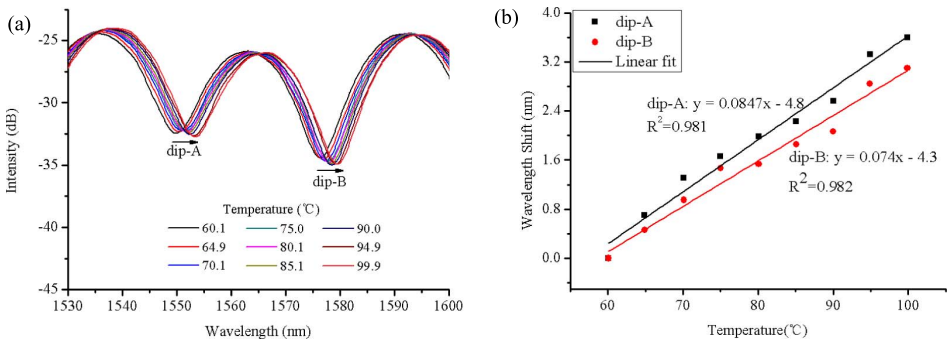

Fig. 6. (a) Transmission spectra of sensor 1 at different temperatures. (b) Wavelength shift of dip-A and dip-B versus the temperature change.

The influence of temperature on the dip wavelength can be expressed by

$$\Delta\lambda_m^T = \left(\delta\frac{L}{2m+1} + \xi\frac{\Delta n_{\text{eff}}^0}{2m+1}\right)\Delta T \tag{4}$$

where δ is the thermo-optic coefficient, ξ is the thermo-expansion coefficient, and ΔT is the variation of temperature. It can be seen that the wavelength shift of the interference fringe is linear to the variation of temperature, and therefore, temperature measurement by using the proposed MZI is expected.

In temperature experiment, the MZI is placed on a heating furnace. The temperature is set from 40 °C to 100 °C with a step of 5 °C, and the transmission spectra are recorded.

Simultaneous measurement of curvature and temperature can be achieved by monitoring the wavelength shift of selected two dips. Since the two dips have different sensitivities towards curvature and temperature, the variations of curvature and temperature can be discriminated, and can be calculated using coefficient matrix as [9]

$$\begin{bmatrix}\Delta C\\ \Delta T\end{bmatrix} = \frac{1}{D}\begin{bmatrix}k_{T,B} & -k_{T,A}\\ -k_{C,B} & k_{C,A}\end{bmatrix}\begin{bmatrix}\Delta\lambda_A\\ \Delta\lambda_B\end{bmatrix} \tag{5}$$

where ΔC is the variation of curvature; $D = K_{C,A}K_{T,B} - K_{C,B}K_{T,A}$, $K_{C,A}$, and $K_{T,A}$ are the curvature and temperature sensitivities of dip-A, respectively; $K_{C,B}$ and $K_{T,B}$ are the curvature and temperature sensitivities of dip-B, respectively; and $\Delta\lambda_A$ and $\Delta\lambda_B$ are the wavelength shift of dip-A and dip-B, respectively.

4. Experimental Results and Discussion

Fig. 5(a) shows the interference fringes of the sensor 1 at the curvature of 4.42 m^{-1}. Dip-A and dip-B are selected at the wavelengths of around 1540 nm and 1571 nm respectively, as they have the maximal contrast ratio. Fig. 5(b) shows that the wavelength of dip-B has a blue shift from 1571.6 nm to 1548.4 nm, and the wavelength of dip-A has a blue shift from 1540.4 nm to 1521.5 nm, when the curvature increases from 4.42 m^{-1} to 5.50 m^{-1}. Fig. 5(c) shows the variations of dip-A and dip-B with different curvatures. It can be seen that the resonant dip-A disappears when the curvature is increased larger than 5.96 m^{-1}. The resonant dip-B can be observed when the curvature is increased to 6.93 m^{-1}, but the contrast ratio is very low, which leads the dip wavelength difficult to read out. Besides, the resonant wavelengths of dip-A and dip-B are according to different interference orders m. Therefore, they show different responses to curvatures. The wavelength shifts of dip-A and dip-B as a function of curvature change are shown in Fig. 5(d). The curvature sensitivities of dip-A and dip-B are obtained by linear fitting and they are −18.166 nm/m^{-1} and −22.227 nm/m^{-1}, respectively. Moreover, the curvature applied is up to about 10 m^{-1} in the experiment. The sensor head can endure the applied

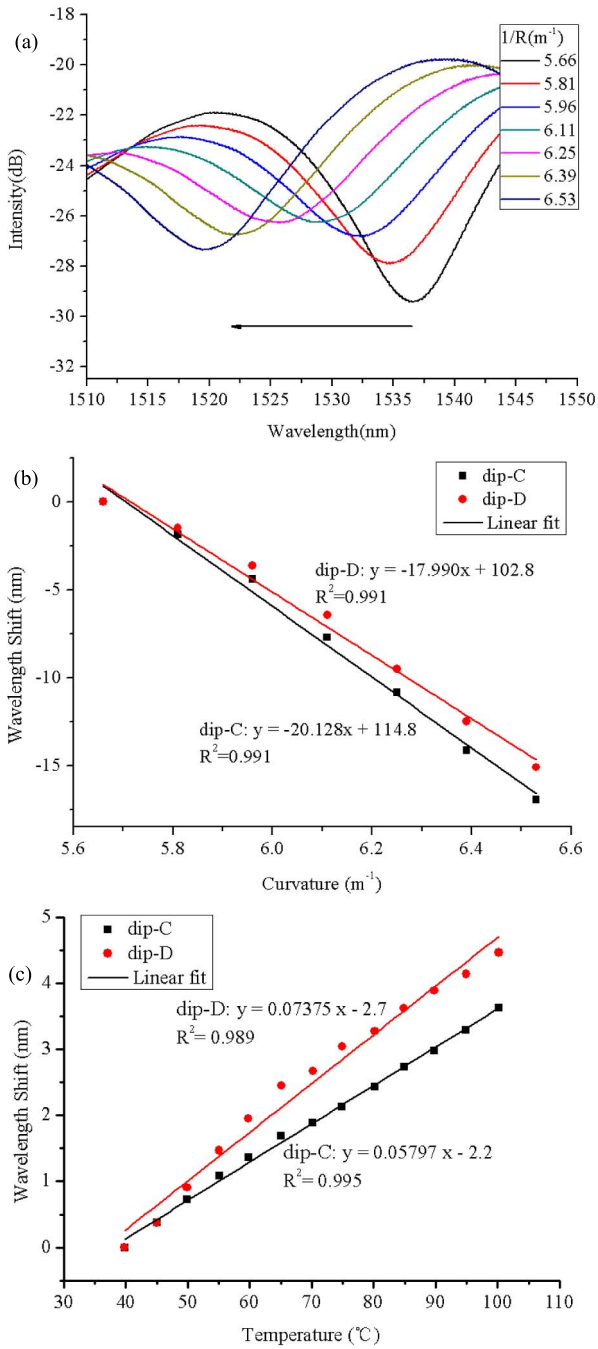

Fig. 7. (a) Wavelength shift of dip-C at different curvatures. (b) Curvature response of sensor 2 (16 mm). (c) Temperature response of sensor 2 (16 mm).

curvature many times and is not easy to break, which means the sensor has high mechanical strength.

Fig. 6(a) shows the transmission spectra at different temperatures. Both dip-A and dip-B have red shift, dip-A has a shift of about 3.5 nm and dip-B has a shift of about 3.1 nm. Fig. 6(b) shows the relationship between temperature variations and the wavelength shifts of dip-A and dip-B. The sensitivities of dip-A and dip-B are 0.0847 nm/°C and 0.074 nm/°C, respectively.

Curvature measurement of sensor 2 with length of 16 mm is also performed. Two wavelength dips of about 1536 nm and 1573 nm are selected as dip-C and dip-D respectively. As the curvature rise from 5.66 m^{-1} to 6.53 m^{-1}, the two dips have blue shift, and the wavelength shift of dip-C is shown in Fig. 7(a). The relationship between curvature and wavelength shift is shown in Fig. 7(b), where the linear fitting results show that the curvature sensitivities are –20.128 nm/m^{-1} and –17.990 nm/m^{-1}, respectively.

Temperature response of sensor 2 is also tested. Fig. 7(c) shows the wavelength shift of the two dips as a function of temperature variations. When the temperature rises from 40 °C to 100 °C, the two dips have a red shift, about 3.6 nm and 4.5 nm, respectively. The measured wavelength shifts with temperature variations are analyzed by linear fitting, and the temperature sensitivity are 0.05797 nm/°C and 0.07375 nm/°C, respectively.

According to (5), the variations of curvature and temperature can be discriminated by coefficient matrix. Substituting the curvature sensitivities and temperature sensitivities of dip-A and dip-B to (5), we can get

$$\begin{bmatrix} \Delta C \\ \Delta T \end{bmatrix} = \frac{1}{0.5383} \begin{bmatrix} 0.074 & -0.0847 \\ 22.227 & -18.166 \end{bmatrix} \begin{bmatrix} \Delta\lambda_A \\ \Delta\lambda_B \end{bmatrix} \tag{6}$$

$\Delta\lambda_A$ and $\Delta\lambda_B$ are the wavelength shift of dip-A and dip-B, respectively. For sensor 2, the simultaneous measurement of curvature and temperature can be achieved by the same way.

The best curvature sensitivity of –22.227 nm/m^{-1} is obtained in the range of 4.42–5.50 m^{-1} for sensor 1 (length of 20 mm), and the corresponding curvature resolution is 9×10^{-4} m^{-1}, which is comparatively high. This sensitivity is higher than that of the sensors in [4]–[6], [8], [9], [12], and is slightly lower than that in [7], but the structure robustness of our sensor is much better. In addition, the temperature sensitivity of 0.0847 nm/°C is higher than that of the sensors in [9], [11], and [13]. Moreover, the fiber used in our sensor is just conventional SMF, and the sensor has the advantages of easy fabrication and low cost when compared with the sensors in [2], [10], and [12].

5. Conclusion

In summary, a novel MZI constructed by core-offset and spherical-shape structures for simultaneous measurement of curvature and temperature is demonstrated. The results show that the wavelength shifts of two selected dips are almost proportional to the variations of curvature and temperature. The curvature sensitivities of sensor 1 (length of 20 mm) are –18.166 nm/m^{-1} and –22.227 nm/m^{-1}, and the temperature sensitivities are 0.0847 nm/°C and 0.074 nm/°C. The curvature sensitivities of sensor 2 (length of 16 mm) are –20.128 nm/$m^{-1}$and –17.990 nm/m^{-1}, and the temperature sensitivities are 0.05797 nm/°C and 0.07375 nm/°C. Sensitivity coefficient matrix can be applied to distinguish the variations of curvature and temperature. The proposed sensor has high curvature sensitivity, so it is suitable for high-accuracy curvature measurement. In addition, it has the advantages of easy fabrication, low cost, and good robustness.

References

[1] J. P. Chen, J. Zhou, and X. C. Yuan, "Mach–Zehnder interferometer constructed by two S-bend fibers for displacement and force measurements," *IEEE Photon. Technol. Lett.*, vol. 26, no. 8, pp. 837–840, Apr. 2014.
[2] T. Y. Huang *et al.,* "A sensitivity enhanced temperature sensor based on highly Germania-doped few-mode fiber," *Opt. Commun.*, vol. 324, pp. 53–57, Aug. 2014.
[3] Y. Zhao, L. Cai, X. G. Li, F. C. Meng, and Z. Zhao, "Investigation of the high sensitivity RI sensor based on SMS fiber structure," *Sens. Actuators A, Phys.*, vol. 205, pp. 186–190, Jan. 2014.
[4] H. P. Gong, H. F. Song, X. R. Li, J. F. Wang, and X. Y. Dong, "An optical fiber curvature sensor based on photonic crystal fiber modal interferometer," *Sens. Actuators A, Phys.*, vol. 195, pp. 139–141, Jun. 2013.
[5] H. P. Gong, X. Yang, K. Ni, C. L. Zhao, and X. Y. Dong, "An optical fiber curvature sensor based on two peanut-shape structures modal interferometer," *IEEE Photon. Technol. Lett.*, vol. 26, no. 1, pp. 22–24, Jan. 2014.
[6] S. S. Zhang, W. G. Zhang, S. C. Gao, P. C. Geng, and X. L. Xue, "Fiber-optic bending vector sensor based on Mach–Zehnder interferometer exploiting lateral-offset and up-taper," *Opt. Lett.*, vol. 37, no. 21, pp. 4480–4482, Nov. 2012.

[7] L. Niu, C. L. Zhao, H. P. Gong, Y. Li, and S. J. Jin, "Curvature sensor based on two cascading abrupt-tapers modal interferometer in single mode fiber," *Opt. Commun.*, vol. 333, pp. 11–15, Dec. 2014.
[8] L. L. Mao, P. Lu, Z. F. Lao, and D. M. Liu, "Simultaneous measurement of curvature and temperature based on Mach–Zehnder interferometer with lateral offset and ultra-abrupt taper," presented at the Conf. Lasers Electro-Optics Pacific Rim, Kyoto, Japan, Jun. 30–Jul. 4 , 2013, Paper ThF2_4.
[9] Y. Zhou *et al.,* "Simultaneous measurement of curvature and temperature based on PCF-based interferometer and fiber Bragg grating," *Opt. Commun.*, vol. 284, no. 24, pp. 5669–5672, Dec. 2011.
[10] Y. P. Wang *et al.,* "Intensity measurement bend sensors based on periodically tapered soft glass fibers," *Opt. Lett.*, vol. 36, no. 4, pp. 558–560, 2011.
[11] M. M. Wang, L. Jiang, S. M. Wang, X. D. Tan, and Y. F. Lu, "A robust fiber inline interferometer sensor based on a core-offset attenuator and a microsphere-shaped splicing junction," *Opt. Laser Technol.*, vol. 63, pp. 76–82, Nov. 2014.
[12] M. Deng, C. P. Tang, T. Zhu, and Y. J. Rao, "Highly sensitive bend sensor based on Mach–Zehnder interferometer using photonic crystal fiber," *Opt. Commun.*, vol. 284, no. 12, pp. 2849–2853, Jun. 2011.
[13] X. L. Xue *et al.,* "Simultaneous measurement of temperature and refractive index using a simplified modal interferometer composed of tilted long-period fiber grating and fiber bitaper," *Meas. Sci. Technol.*, vol. 24, no. 6, May 2013, Art. ID 065103.